Effect of graphene on microstructure and properties of copper paste

YINHU QU*, XIAONI LIU, YI LIU, JINGJING SHI, XIAOLE CHENG, ZONGTUAN ZHOU
School of Mechanical and Electronic Engineering, Xi'an Polytechnic University, Shaanxi, Xi'an 710048, China

The microstructure, resistances and composition of graphene-copper composite paste were studied by means of scanning electron microscope (SEM), four point probe tester and X-ray diffraction (XRD). The rheological behavior and conductive mechanism of the composite paste were analyzed, and the geometric model of connection of conductive phase was established. The results indicate that the resistance decreases firstly and then increases sightly with the increasing content of graphene. When the mass ratio of graphene to copper powders is 3:97, the resistance of the prepared composite paste with 5μm graphene sheets reaches to the minimum value of 2.68 mΩ·cm, which is decreased by 92.22% in comparison with copper paste. The conductive film surface of this graphene-copper composite paste is flatter and denser than that of copper paste, forming the closer contact among conductive phases. During the cooling process, surface tension of glass liquid causes pores between the copper powders and graphene shrunk to promote the rearrangement of copper powder and graphene, resulting in more conductive phase contacted compactly, and finally forming a chain structure and excellent conductive network. In the conductive film, the shorter graphene will fill into gaps among copper powders and longer graphene will form a "cross-bridge". This would be in favor of building a conductive path and promoting the conductivity of the conductive paste.

(Received February 14, 2018; accepted February 12, 2019)

Keywords: Graphene, Copper powders, Conductive paste, Resistance

1. Introduction

Conductive paste, as an electronic functional material with high technology and high performance, is the basic material for thick film components and widely used in electronics, information, communications and other industries. As the precision and miniaturization of electronic devices, high quality conductive pastes have drawn more and more attention of the researchers [1–4]. Conductive paste is mainly composed of conductive phase, organic carrier and binder. The conductive phase determines largely the conductivity of the paste, and affects the physical and mechanical properties of the conductive film [5,6]. In traditional conductive paste, noble metal is often used as conductive phase, which makes the paste have excellent conductivity and stability. Conductive paste such as gold paste and silver paste has been investigated extensively. As is known to all, Ag has excellent conductivity and stable chemical properties, but it's very expensive. In addition, the migration of Ag^+ occurs in the process of application, which leads to reduction in performances of the components and then restricts its application. The conductivity of Au is excellent, but its cost is more expensive than Ag, so it is not a good way to be used for industrialized production. Copper has a wide range of sources and its conductivity is close to that of Ag (the resistance of Ag is 1.59×10^{-6} Ω·cm, and the resistance of Cu is 1.72×10^{-6} Ω·cm at 20°C). In addition, its cost is only 1/100-1/120 of silver. Therefore, it is an ideal conductive phase for preparing conductive paste. It is a pity that the copper is easy to be oxidized in air and forms an oxide film on the surface, resulting in a decline of conductivity of copper [7–10]. In recent years, researchers in many countries have made a lot researches about surface oxidation resistance of copper powders [11–13]. For instance [14–16], oxidation resistance of electroless silver coating on fine copper powders is investigated, the results show that the sheet resistances of metal films reduce with the increasing silver content and present the improvement of oxidation resistance. Based on that, silver-coated copper powders are prepared making use of the substitution reaction between copper and silver, and finally the properties of oxidation resistance are improved. In addition, the study also shows that copper powders are pre-coated in mixed solution of methanol and oleic acid, and then SiO_2–Al films are coated secondly on the copper powders by sol-gel method under protection of the Ar. With in this mind, this paper applies the method that copper powders coated with acrylic resin are used as conductive phase. In recent years, graphene has shown great potential in many fields, such as transistors, sensors, biomedicine, solar cell and so on, especially as a conductive reinforcing phase to join composite paste due to its excellent physical properties [17-19], the application of graphene in the field of composite materials has attracted much attention of researchers. Electron mobility of graphene is more than 15000 $cm^2/V\cdot s$ at room temperature and is higher than that of carbon nanotubes or silicon crystals, but its resistance is only 10^{-8} Ω·cm, far lower than copper or silver [20]. Thus, addition of

graphene is expected to greatly improve the conductivity of copper composite paste.

2. Experiment

2.1. Pre-treatment of copper powders

The copper powders were coated with acrylic resin, and the operation steps were as follows: first, copper powders were scoured by hydrochloric acid with a mass fraction of 8%, and then were scrubbed by deionized water for 2-3 times, until there was no obvious odour of hydrochloric acid; second, acrylic resin was used as wall material, and it integrated into organic solvent of acetone and ethyl acetate to prepare microcapsule solution; third, the pretreated copper powders were coated by microcapsule solution; the last, under the atmosphere of nitrogen, the copper powders were put in self-propagating synthesis reactor, and was subsequently heated to 50°C for 2h with the speed of 10°C/min.

2.2. Preparation of graphene-copper composite paste and conductive film

Preparation process of graphene-copper composite paste was shown in Fig. 1. The organic carrier (Table 1) was prepared by terpineol, ethyl cellulose, defoaming agent, silane coupling agent and ethyl acetate. The coated copper powders were mixed with graphene, glass powders (as binder, its melting temperature is 430°C) and organic carrier. Thereinto, the organic carrier and glass powders respectively accounted for 22% and 8% of the paste. Graphene-copper composite paste was obtained subsequently by stirring and high-energy grinding for the above mixture. The graphene-copper composite paste was printed to α-Al_2O_3 substrate according to the standard of GB1727-1992 and GB4054-2008 aimming to measure the properties of paste. The processes were as follows: firstly, α-Al_2O_3 substrate was cleaned with anhydrous alcohol; secondly, the paste was printed on the α-Al_2O_3 substrate by manual screen printing; thirdly, printed film of paste was sintered in the self-propagating synthesis reactor to 470°C for 20min, the thickness of sintered conductive film was 20±3μm. After cooled for 1-2 hours, performances of conductive film were tested.

2.3. Characterizations and measurements

Microstructure observation was performed by JSM-6700F scanning electron microscopy (SEM). The scanning electron microscopy was operated at 5kV using a working distance of 10.7 mm. Phase analysis was carried on a D/max2200Pc type of X-ray diffractometer with Cu-Ka radiation at 40 kV and 40mA. The samples were scanned in the 2θ range of 20-80°and with a scan rate of 0.02 deg/s. The resistance was measured by using a four point resistance measurement method to examine 5 random dots on the surface.

Table 1. The composition and proportion of organic carrier (wt%)

Ethyl Cellulose	Terpilenol	Defoamer Agent	Silane Coupling	Ethyl Acetate
4.75	82.18	2.57	5.37	5.13

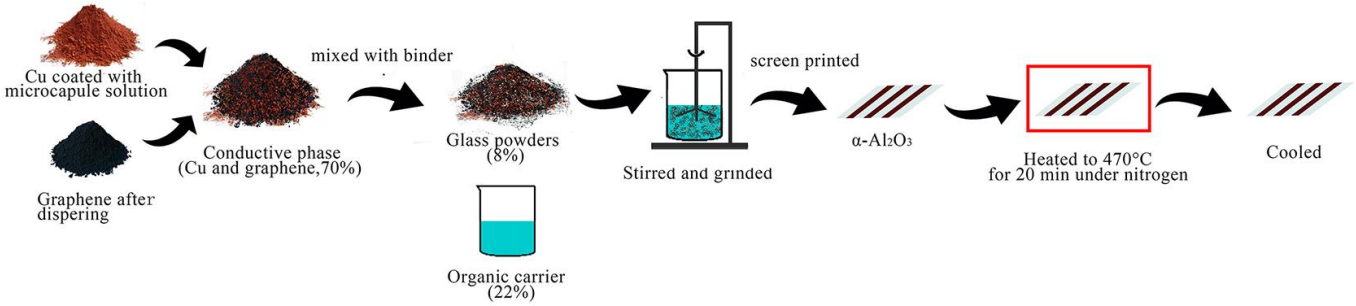

Fig. 1. Preparation process of graphene-copper composite paste

3. Results and discussion

3.1. Characterizations of the copper powders

Fig. 2 shows the XRD pattern of copper powders coated with acrylic resin and laid ten days in the air. The diffraction peaks at 2θ=43.25°, 50.37° and 73.99° correspond to the (111), (200) and (220) crystal planes of copper, respectively. The diffraction peaks of Cu_2O or CuO are found, which reveals copper powders coated with acrylic resin have excellent anti oxidation property.The surface morphology of the uncoated copper powders and coated copper powders are shown in Fig. 2. As can be seen, uncoated copper powders aggregate seriously, this indicates the dispersion of uncoated copper powders is poor and it will seriously affect the conductivity of the paste (Fig. 3(a)). Likewise, the dispersion of coated copper powders is improved and the size of aggregates is decreased as shown in Fig. 3(b).

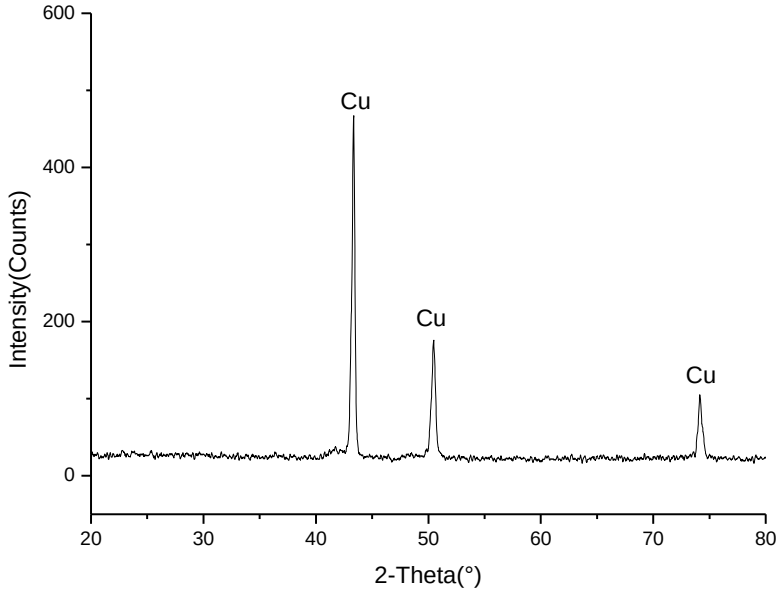

Fig. 2. XRD pattern of copper powders

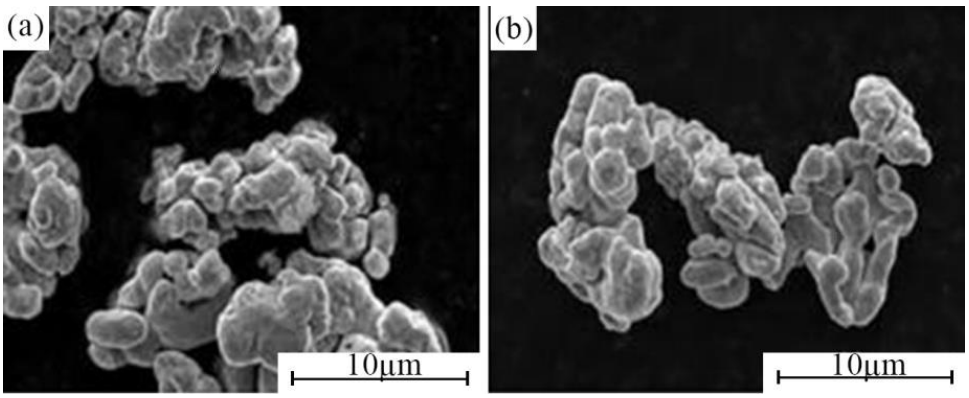

Fig. 3. Surface morphology of the copper powders: (a) uncoated, (b) coated with acrylic resin

3.2. Effect of graphene content on the resistance of the paste

Graphene (the size of sheets is 1μm) is used as conductive reinforcing phase, the mass ratio of graphene to copper powders is determined by varying graphene content. Fig. 4 represents that the resistance of the graphene-copper composite paste decreases sharply by adding graphene. This indicates the addition of graphene enhances the conductivity of copper composite paste, and the enhancement effect is related to graphene content. As the graphene content increasing, the resistance of the composite paste decreases firstly and then increases. One reason for this is that graphene is a kind of nano-material with low density and high conductivity, and a bit of graphene can act as media to connect copper powders, so the resistance of the paste is decreased at the beginning. However, along with the increasing of graphene content, its volume is too larger to disperse, and uneven grinding maybe exists during paste preparation, these cause the paste uneven and viscosity increased. Therefore, excessive amount of graphene can lead to poor printing performance. The results also show that resistance reaches to the minimum value of 6.81 mΩ·cm when the mass ratio of graphene to copper powders is 3:97, the composite paste has the best conductivity under this condition.

The microstructures of copper paste and graphene-copper composite paste are shown in Fig. 5. From Fig. 5(a) and 5(b), it can be seen that there are a lot of holes on the surface of copper paste, and loose contact or less contact among copper powders. The copper powders are dispersed and precipitated in the glass liquid though sintering. A small amount of glass powders is filled in the pores of copper powders, and the paste is sintered on the substrate to form the film. However, the effective conductive path has not been established because glass powders have no conductivity. It can be seen from Fig. 5(c) and 5(d) that the surface of conductive film is flatter and denser than that of copper paste, at the same time less holes and closer contact among conductive phase are observed. Graphene can be evenly distributed and has no or rarely agglomeration. Furthermore, shorter graphene can fills in

the pores of copper powders and longer graphene can build "cross-bridge", these all have a positive effect on electrical conductivity. In addition, the thermal conductivity of copper and graphene is about 24000J/ (M. K. S)) and 5300J/ (M. K. S) respectively, and copper and graphene can both cause thermal vibration or internal electron migration, these form tunneling current and improve electrical conductivity.

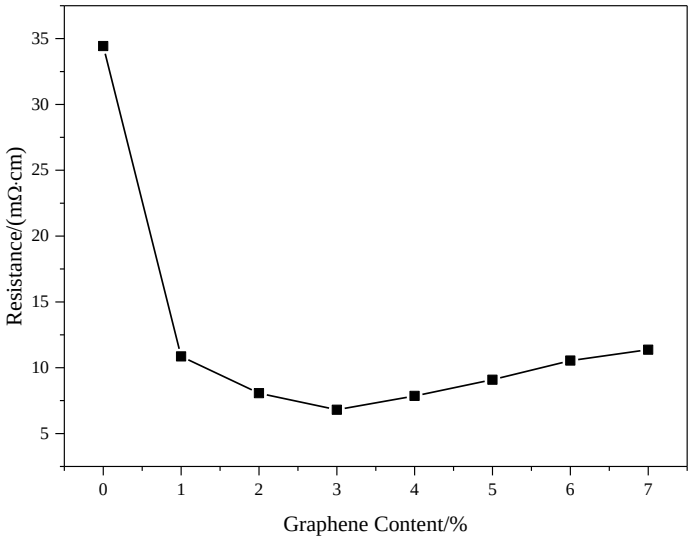

Fig. 4. Effect of graphene content on the resistance of the paste

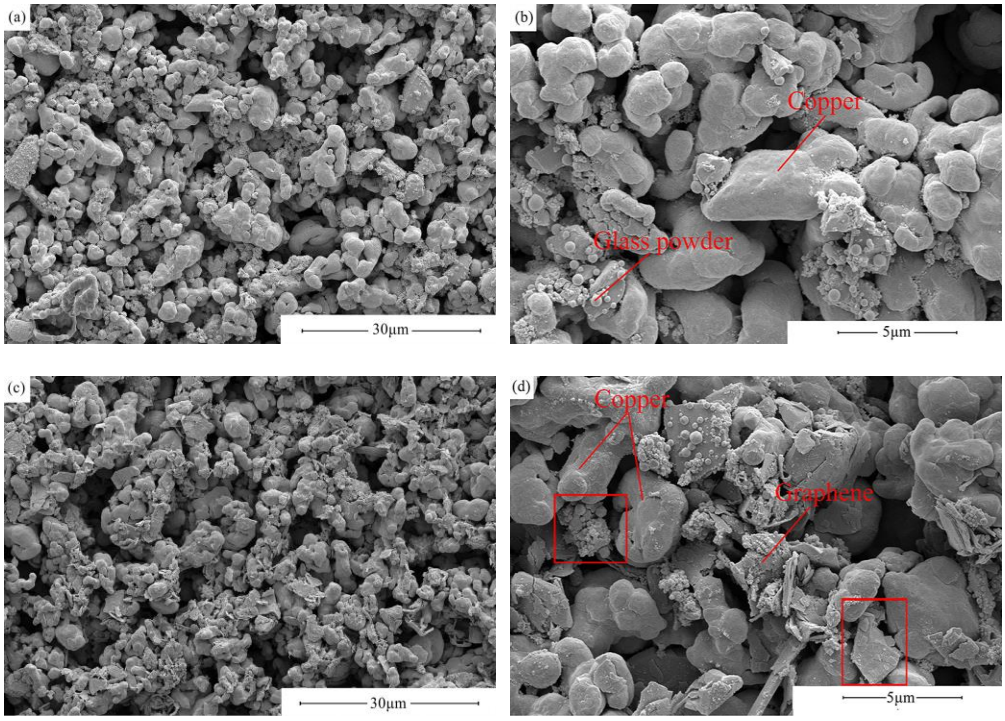

Fig. 5. Microstructure of the copper paste: (a,b) no graphene, (c,d) graphene content with 3wt%

3.3. Effect of size of graphene sheet on the resistance of paste

As shown in Table 2, the resistance of the paste is also related to size of graphene sheets. Resistances of pastes decrease firstly and then increase as the size of graphene sheets increasing. Resistances of paste prepared with 5μm graphene sheets is 2.68 mΩ·cm, which is decreased by 92.22% in comparison with that of the copper paste. This is because graphene sheets with smaller size and fewer number of layers have excellent conductivity. The thinner thickness and the more number graphene sheets are, the more opportunities that graphene sheets fill the pores among copper powders and form the conductive network in the paste, which decreases the resistance of the paste. On the contrary, if the size of graphene sheets are too large,

even more than the size of copper powders, to fill the pores among copper powders, leading to a small reduction in resistance compared with the paste prepared with 5μm graphene sheets.

Table 2. Resistances of the pastes with different sizes of graphene sheets and reduction rate compared with copper paste

Size of graphene sheets /μm	1	5	8	10	25
Resistance /(mΩ·cm)	6.81	2.68	3.52	4.03	22.91
Reduction rate /%	80.22	92.22	89.78	88.30	33.46

SEM images of the pastes with different sizes of graphene sheets are shown in Fig. 6 (all the magnifications are 20000×). Fig. 6(a) is copper paste prepared with 1μm graphene sheets, the size of graphene sheets is the smallest in the five kinds of graphene, and most of them could be able to fill in the pores. However, due to larger thickness of 1μm graphene sheets, the number that filling in the pores of copper powders is less than other sizes of graphene sheets when qualities of five kinds of graphene sheets are same. Thus, the resistance is higher. In addition, the size of graphene sheets is far larger than that of copper powders (as shown in Fig. 6(c)), this results in building connection between copper powders surface and graphene sheets, but graphene sheets are difficult to be filled in the pores among copper powders to form conductive network. In Fig. 6(b), the size of graphene sheets are 5μm. The mixture of copper powders and graphene is ground by high-energy grinder in preparation of the paste, which causes the size of graphene sheets reduces. So it is able to be filled among copper powders and connect copper powders. Therefore, complete conductive path is built. Subsequently, the composition of the graphene-copper composite paste is measured by XRD, and rheological behavior and density are also analyzed.

3.4. Analysis of conductive mechanism

According to the above discussion, geometric models about the conductive phase of graphene-copper composite paste are established (shown in Fig. 7). Before sintering, the copper powders, graphene sheets and glass powders are mostly dispersed in the organic carrier without contact each other, and the conductive path is not formed. The organic carrier is completely volatilizes, and the glass powders is melted into glass liquid by absorbing heat continuously during sintering. During the cooling process, surface tension of glass liquid causes pores between the copper powders and graphene shrunk to promote the rearrangement of copper powder and graphene, resulting in more conductive phase contacted compactly, and finally formation of a chain structure. This would be in favor of building a conductive path and promoting the conductivity of the conductive paste.

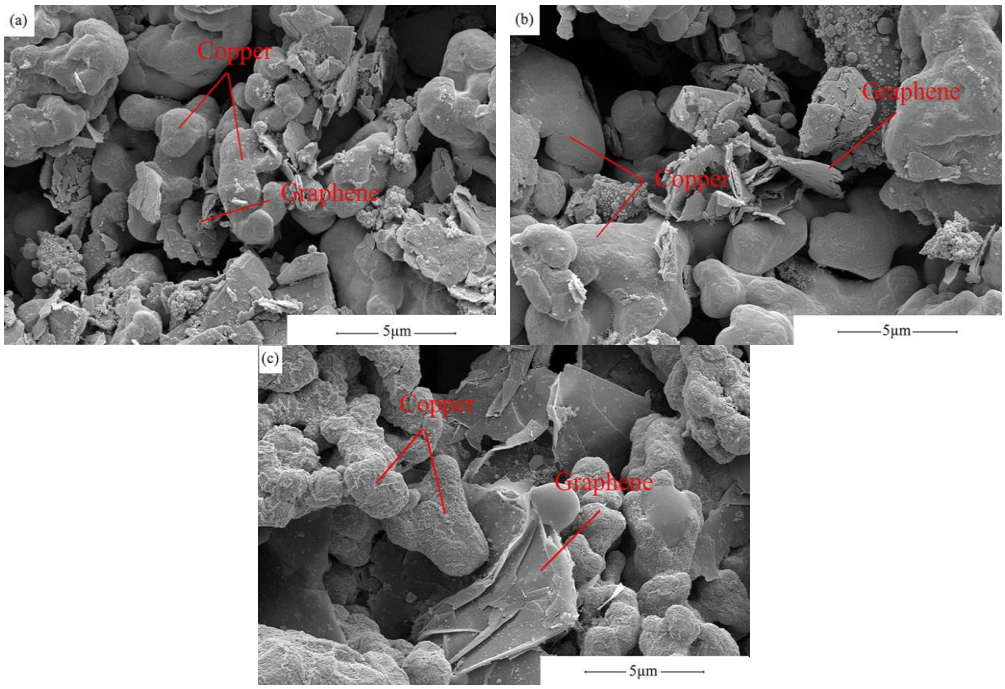

Fig. 6. Microstructure of copper composite paste prepared with different sizes of graphene: (a) 1μm graphene sheets, (b) 5μm graphene sheets, (c) 25μm graphene sheets

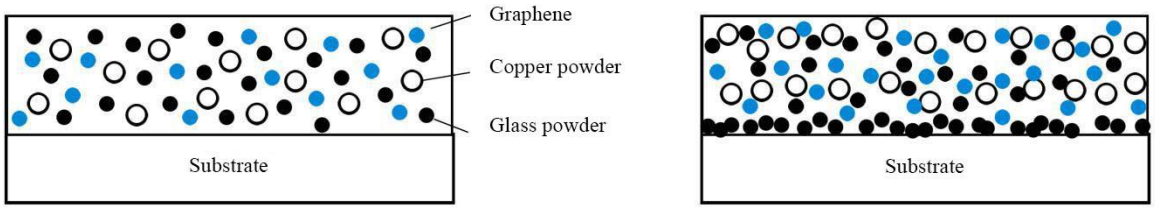

(a)The composite paste after printing *(b) The composite paste after sintering*

Fig. 7. Geometric models of graphene-copper composite paste

3.5. XRD of the composite paste

The X-ray diffraction (XRD) pattern of the graphene-copper composite paste is shown in Fig. 8. From Fig. 8, it is found that the profiles of the diffraction peaks are quite narrow, and diffraction peaks consist of Cu, C and Al_2O_3 without any copper oxide peaks such as Cu_2O and CuO. This result reveals that the copper powders isn't oxidized in the process of paste preparation and conductivity of graphene-copper composite paste isn't affected. The main diffraction peak is Cu and a weak diffraction peak of C can be seen. In addition, the Al_2O_3 peak is found due to X-ray penetration through sintering film.

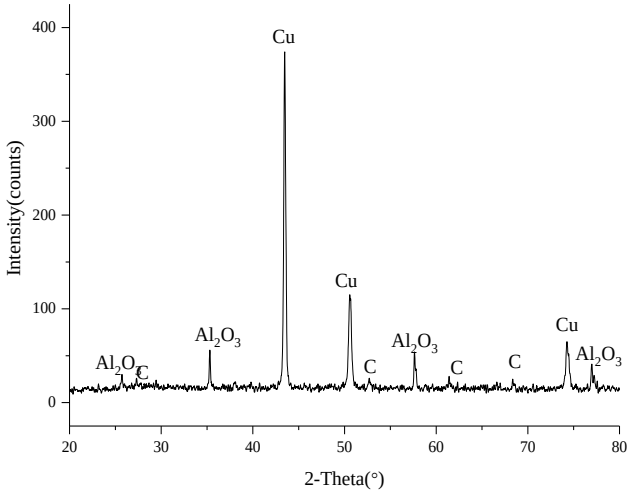

Fig. 8. XRD pattern of graphene-copper composite paste (sintered at 470°C)

3.6. Rheological behavior of the composite paste

In order to ensure excellent fluidity, printability and structural integrity (without delamination and deformation) during drying and sintering, the rheological behavior of the graphene-copper composite paste must be analyzed. Effect of shear rate on the viscosity and shear stress of the paste is shown in Fig. 9. It can be observed that the paste has obvious shear thinning behavior, and the viscosity fluctuates in the range of 2.59-1590 Pa·s under different shear rates. As the shear rate increasing, the shear stress values are within the range of 41.5-965Pa, which presents a trend of increasing firstly and then decreasing. This shows that a little shear force is necessary to obtain the flat printed surface during screen printing and the paste has excellent rheological behavior.

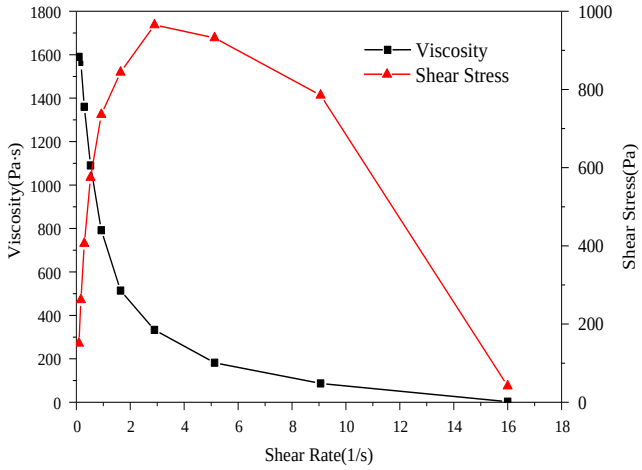

Fig. 9. Effect of shear rate on the viscosity and shear stress of the paste

3.7. Calculation of density

The actual density of the paste is measured by Archimedes method. Its theoretical density is calculated by the formula of $\rho = \sum v_i \rho_i$, Thereinto, v_i in formula is the volume fraction of materials, and ρ_i is the density of materials. Thus, density percentage and porosity of the paste are obtained and as shown in Table 3 and Table 4. The porosity of the paste is reduced after adding graphene and the density is improved after sintering. This is because that the conductive film after printing is relatively soft, conductive phase contacts loosely, resulting in poor conductive properties. But shrinkage deformation of the conductive film after sintering leads to fine and close contact among conductive phases and decreases porosity, the conductivity of the composite paste is improved finally significantly.

Table 3. Density of pastes after printing

Sample	Actual density after printing /(g·cm^{-3})	Theoretical density /(g·cm^{-3})	Density percentage /%	Porosity /%
Copper paste	1.03	1.38	74.64	23.36
Graphene-copper paste	1.09	1.40	77.86	22.14

Table 4. Density of pastes after sintering

Sample	Actual density aftersintering /(g·cm^{-3})	Theoretical density /(g·cm^{-3})	Density percentage /%	Porosity /%
Copper paste	1.84	2.34	78.63	21.37
Graphene-copper paste	1.25	1.56	80.13	19.87

4. Conclusions

(1) As the graphene content increasing, the resistance of the composite paste decreases firstly and then increases. When the mass ratio of graphene to copper powders is 3:97, the resistance of the composite paste reaches to the minimum value.

(2) The resistance of composite paste is also related to size of graphene sheets and decreases firstly and then increases as the size of graphene sheets increasing. The lowest resistance of the composite paste prepared with 5μm graphene sheets is 2.68 mΩ·cm.

(3) Through analysing conductive mechanism, we found that the small graphene sheets could fill pores among the copper powders and the longer graphene sheets could build a "cross-bridge" among copper powders, which increased the connection of the conductive phase and improved the conductivity of the paste.

Acknowledgments

The authors would like to thank the financial support for this work from Shaanxi Science and Technology Research and Development Program Projects under (2013K09-33), Xi'an Science and Technology Plan Projects under 2017074CG/RC037(XAGC002) and 2017074CG/RC037 (XAGC007), and thank the Institute of Collaborative Innovation Center of Xi'an Polytechnic University for providing help in testing relevant properties.

References

[1] T. Shi, H. Qi, B. Yan, Shanghai nonferrous metals **33**(3), 145 (2012).
[2] I. Mir, D. Kumar, Int. J. Adhes. Adhes. **28**(7), 362 (2008).
[3] V. A. Rozenenkova, S. S. Solntsev, N. A. Mironova, Glass Ceram. **70**(7-8), 269 (2013).
[4] H. K. Chikusei, J. K. Bangkok. Conductive paste. Patent US7718090B2, United State, 18 May, 2013.
[5] J. Putaala, M. Sobocinski, S. Ruotsalainen, J. Juuti, P. Laakso, H. Jantunen, Opt. Lasers Engng. **56**, 19 (2014).
[6] M. Kajita, T. Takahashi, A. Kano, T. Sato, Trans. Jpn. Inst. Electron. Packag. **8**(1), 151 (2015).
[7] M. Yoshida, H. Tokuhisa, U. Itoh, T. Kamata, I. Sumita, S. Sekine. Energy Procedia **21**, 66 (2012).
[8] C. Clementa, H. Bella, F. Vogga, L. Rebenklaub, P. Gierthb, U. Partscha, Energy Procedia **38**, 423 (2013).
[9] D. Wood, I. Kuzma-Filipek, R. Russell, F. Duerinckx, N. Powell, A. Zambova, B. Chislea, P. Chevalier, C. Boulord, A. Beucher, N. Zeghers, J. Szlufcik, G. Beaucarne, Energy Procedia **67**, 101 (2015).
[10] X. Liu, Y. Qu, H. Zheng, X. Jiang, Applied Chemical Industry **43**(8), 1493 (2014).
[11] G. D. Sulka, M. Jaskula, Hydrometallugy **64**(1), 13 (2002).
[12] S. J. Oh, J. H. Lee, Micro Nano Lett. **12**(10), 717 (2017).
[13] R. Zhang, K. Moon, W. Lin, C. P. Wong, J. Mater. Chem. **20**(10), 2018 (2010).
[14] X. Xu, X. Luo, H. Zhuang, W. Li, B. Zhang, Mater. Lett. **57**(24-25), 3987 (2003).
[15] X. Cao, H. Zhang, Powder Technol. **226**, 53 (2012).
[16] S. Chee, J. Lee, J. Mater. Chem. C **2**(27), 5372 (2014).
[17] C. K. Leong, D. D. L. Chung, Carbon. **41**(13), 2459 (2003).
[18] A. K. Geim, Science. **10**, 1530 (2009).
[19] A. A. Balandin, S. Ghosh, W. Z. Bao, I. Calizo, D. Teweldebrhan, F. Miao, C. N. Lau, Nano Lett. **8**(3), 902 (2008).
[20] L. Dong, W. Chen, C. Zheng, N. Deng, J. Alloys Compd. **695**, 1637 (2017).

*Correspondence author: quyinhu@xpu.edu.cn